Brief Communication

Cell Chemical Biology

Mapping Proteome-wide Targets of Glyphosate in Mice

Graphical Abstract

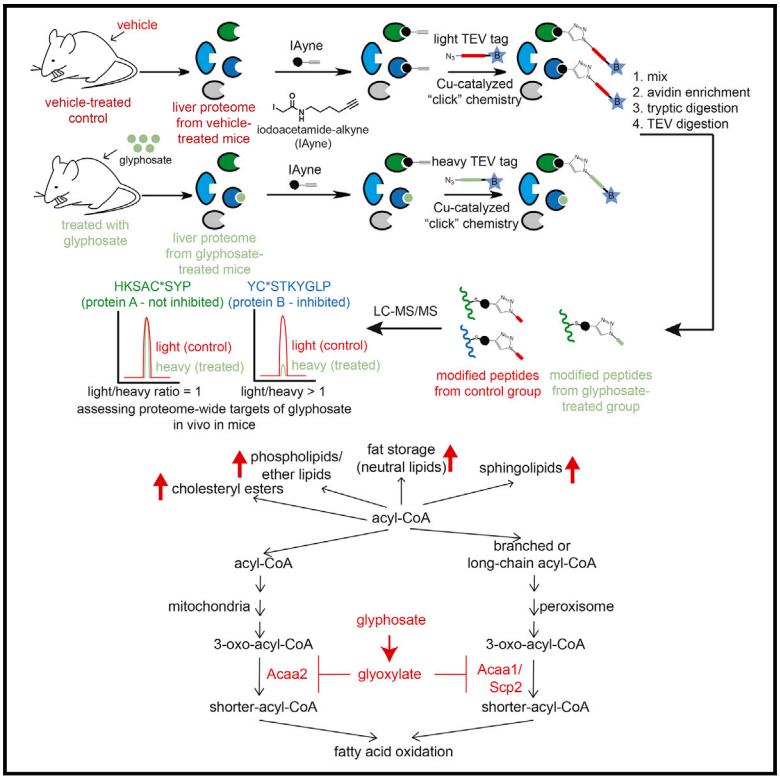

Highlights

- Mechanisms of toxicity for the herbicide glyphosate are not well understood
- We used activity-based protein profiling to look for glyphosate targets in mice
- Glyphosate is metabolized to glyoxylate and reacts with cysteines on liver proteins
- Glyoxylate inhibits fatty acid oxidation and glyphosate increases liver fat

Authors

Breanna Ford, Leslie A. Bateman, Leilani Gutierrez-Palominos, Robin Park, Daniel K. Nomura

Correspondence

dnomura@berkeley.edu

In Brief

Ford et al. show that glyphosate is metabolized to reactive metabolites that inhibit fatty acid oxidation and increase liver triglyceride and cholesteryl ester levels.

Ford et al., 2017, Cell Chemical Biology *24*, 133–140
February 16, 2017 © 2016 Elsevier Ltd.
http://dx.doi.org/10.1016/j.chembiol.2016.12.013

Please cite this article as: Ford et al., Mapping Proteome-wide Targets of Glyphosate in Mice, Cell Chemical Biology (2016), http://dx.doi.org/10.1016/j.chembiol.2016.12.013

Cell Chemical Biology
Brief Communication

Mapping Proteome-wide Targets of Glyphosate in Mice

Breanna Ford,[1] Leslie A. Bateman,[1] Leilani Gutierrez-Palominos,[1] Robin Park,[2] and Daniel K. Nomura[1,3,*]
[1]Departments of Chemistry, Molecular and Cell Biology, and Nutritional Sciences and Toxicology, University of California, Berkeley, 127 Morgan Hall, Berkeley, CA 94720, USA
[2]Integrated Proteomics Applications, Inc., 12707 High Bluff Drive Suite 200, San Diego, CA 92130, USA
[3]Lead Contact
*Correspondence: dnomura@berkeley.edu
http://dx.doi.org/10.1016/j.chembiol.2016.12.013

SUMMARY

Glyphosate, the active ingredient in the herbicide Roundup, is one of the most widely used pesticides in agriculture and home garden use. Whether glyphosate causes any mammalian toxicity remains highly controversial. While many studies have associated glyphosate with numerous adverse health effects, the mechanisms underlying glyphosate toxicity in mammals remain poorly understood. Here, we used activity-based protein profiling to map glyphosate targets in mice. We show that glyphosate at high doses can be metabolized in vivo to reactive metabolites such as glyoxylate and react with cysteines across many proteins in mouse liver. We show that glyoxylate inhibits liver fatty acid oxidation enzymes and glyphosate treatment in mice increases the levels of triglycerides and cholesteryl esters, likely resulting from diversion of fatty acids away from oxidation and toward other lipid pathways. Our study highlights the utility of using chemoproteomics to identify novel toxicological mechanisms of environmental chemicals such as glyphosate.

INTRODUCTION

Glyphosate, the active ingredient in Roundup, is the most commonly used pesticide in the United States across agricultural and home garden use, with 180–185 million pounds used in the United States in 2007 (Grube et al., 2011). Glyphosate is also one of the most controversial herbicides, due to major disagreements about its safety and toxicity (Cressey, 2015; Monsanto, 2015). Many studies have associated glyphosate exposure with various adverse health effects (El-Shenawy, 2009; Samsel and Seneff, 2015), including cancer, liver damage, and dyslipidemia in mammals, and it was recently deemed a probable human carcinogen by the International Agency for Research on Cancer (International Agency for Research on Cancer, 2015; Portier et al., 2016). Understanding how glyphosate interacts with biological systems in vivo in mammals is necessary to assess the prolonged effects and mechanism of toxicity of glyphosate on human health.

There have been previous efforts to characterize the toxicological mechanisms of glyphosate including acute and long-term toxicity studies in animal models, epidemiological studies in human populations, and modern systems biology approaches to map gene expression changes (Chang and Delzell, 2016; El-Shenawy, 2009; Greim et al., 2015; Mesnage et al., 2015; Portier et al., 2016; Samsel and Seneff, 2015). However, many of these approaches have been largely correlative and have likely still missed subtler or indirect pathological effects that may arise from long-term exposures. We believe that understanding the direct chemical-protein interactions of glyphosate or its metabolites will inform our understanding of downstream molecular, metabolic, and pathophysiological effects, providing a more direct approach toward understanding toxicological mechanisms of this widely used pesticide. In this study, we have mapped glyphosate metabolism, targets, and downstream metabolic consequences in vivo in mice toward better understanding the actions of glyphosate in complex biological systems.

RESULTS AND DISCUSSION

Of concern is whether glyphosate may be biotransformed into electrophilic metabolites, which may in turn react with nucleophilic amino acid hotspots on proteins such as cysteines and lysines, which may cause disruptions in protein biochemistry, such as enzyme catalysis, post-translational regulation, redox balance, metal binding, and protein-protein interactions. Glyphosate has been reported to be metabolized by soil microbes and possibly in mammals to aminomethylphosphonic acid (AMPA) and the reactive metabolite glyoxylate (Samsel and Seneff, 2015). Glyoxylate is an aldehyde known to react with nucleophilic amino acids on protein targets, such as cysteines, lysines, and arginines (Gohre et al., 1987; Schuette, 1998).

To determine whether glyphosate is potentially biotransformed into glyoxylate in mammals, we administered isotopic [^{13}C/^{15}N] glyphosate to mice at a high dose of 200 mg/kg intraperitoneally (i.p.), once per day over 7 days, and measured isotopically labeled [^{13}C/^{15}N]glyphosate, [^{15}N]AMPA, and [^{13}C]glyoxylate levels ex vivo in mouse liver using single-reaction monitoring (SRM)-based liquid chromatography-mass spectrometry (LC-MS/MS) derived from fragmentation and retention times of standards for each chemical. We acknowledge that these doses are much higher than exposure levels encountered by the public, but toxicological testing studies with pesticides are oftentimes

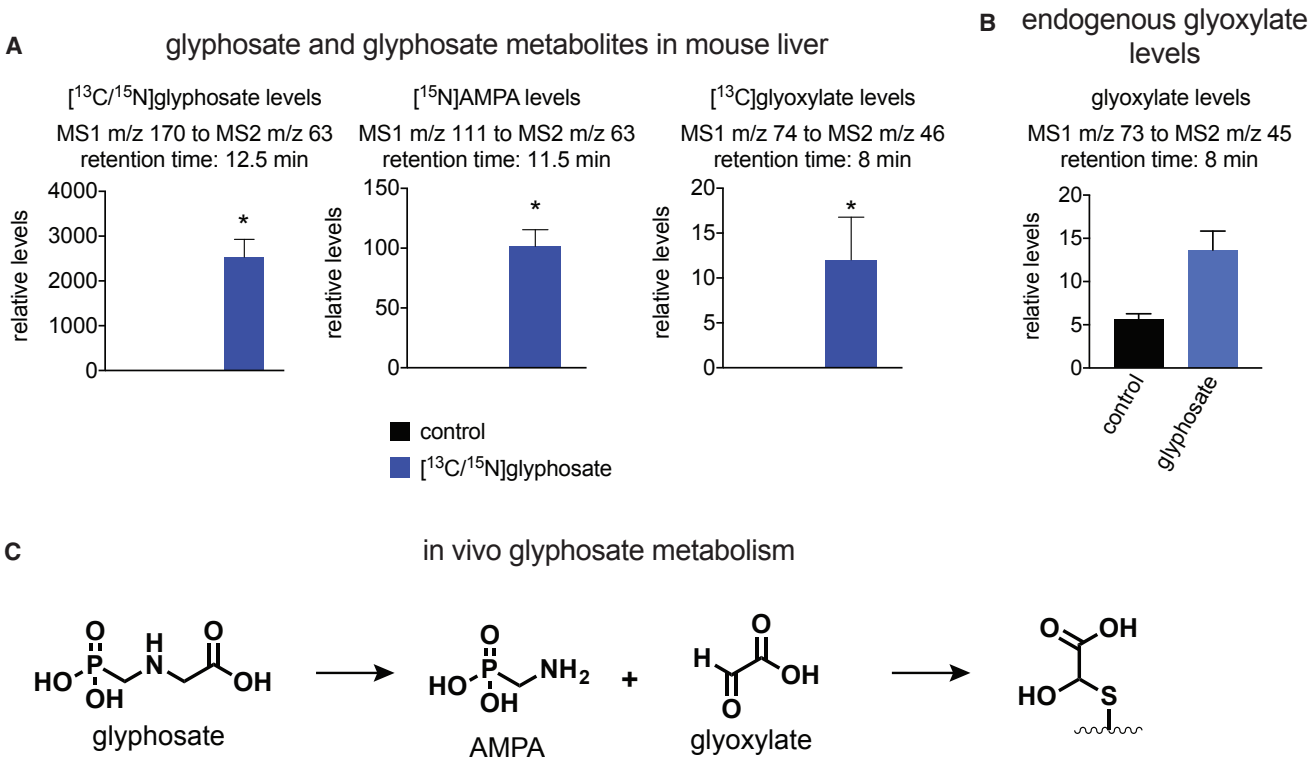

Figure 1. Metabolism of Glyphosate in Mice

(A) Mice were treated with [^{13}C/^{15}N]glyphosate (200 mg/kg i.p., once per day for 7 days) after which livers were harvested and SRM-based LC-MS/MS was used to determine glyphosate, AMPA, and glyoxylate levels.

(B) Mice were treated with nonisotopic glyphosate (200 mg/kg i.p. once per day for 7 days) after which nonisotopic total glyoxylate levels were measured by SRM-based LC-MS/MS.

(C) Our data point to metabolism of glyphosate to AMPA and glyoxylate. Glyoxylate can potentially react with nucleophilic amino acid hotspots such as cysteines and lysines.

Data are presented as mean ± SEM, n = 4 or 5/group. Significance is presented as *$p < 0.05$ compared with vehicle-treated controls.

performed at maximum tolerated doses. Despite previous reports claiming that glyphosate is largely not metabolized in vivo (Williams et al., 2000), we show significant formation of isotopic AMPA and glyoxylate in livers from [^{13}C/^{15}N]glyphosate-treated mice (Figure 1A). The level of glyoxylate formed is approximately 4% of glyphosate levels detected in the liver. Glyoxylate is also produced through various metabolic pathways in mammals, such as glycine degradation (Wang et al., 2013). We also treated mice with nonisotopic glyphosate (200 mg/kg i.p., once per day over 7 days) and show that glyphosate treatment significantly increases glyoxylate levels by ~2-fold above endogenously generated levels at the doses used in this study (Figure 1B).

We postulated that the observed heightened levels of glyoxylate would lead to more glyoxylate reactivity with susceptible nucleophilic residues on proteins in vivo in mice (Figure 1C). To determine whether glyphosate metabolites formed in vivo may affect proteome reactivity, we performed a series of chemoproteomic profiling experiments using reactivity-based probes and activity-based protein profiling (ABPP), a chemoproteomic strategy that uses active-site or reactivity-based chemical probes to map reactive, functional, and ligandable hotspots directly in complex proteomes (Figure 2A) (Counihan et al., 2015; Roberts et al., 2016). When used in a competitive manner, reactive chemicals can be competed against reactivity-based probes to map their proteome-wide reactivity (Counihan et al., 2015; Roberts et al., 2016). First, we performed gel-based ABPP studies in which we determined general cysteine reactivity in mice treated with vehicle or glyphosate by labeling mouse liver proteomes with the cysteine-reactive iodoacetamide-alkyne (IAyne) probe, followed by appendage of rhodamine-azide by copper-catalyzed click chemistry and in-gel fluorescence analysis. We show that in vivo glyphosate treatment selectively reduced cysteine reactivity of several protein targets in mouse liver (Figure 2B; Figure S1). To determine the identity of these targets, we next performed an ABPP proteomic experiment, in which we enriched IAyne-labeled proteins from vehicle- and glyphosate-treated mouse liver proteomes through biotin-conjugation to probe-labeled proteins, avidin enrichment, and proteomic analysis. Of 340 IAyne-enriched proteins, we observed 51 protein targets that showed significantly less IAyne enrichment in glyphosate-treated mouse livers, compared with vehicle-treated controls, indicating that these targets possessed cysteines that were bound by reactive metabolites of glyphosate (Figure 2C; Table S1).

To gain an in-depth understanding of which specific cysteines on proteins were particularly susceptible to in vivo reactive

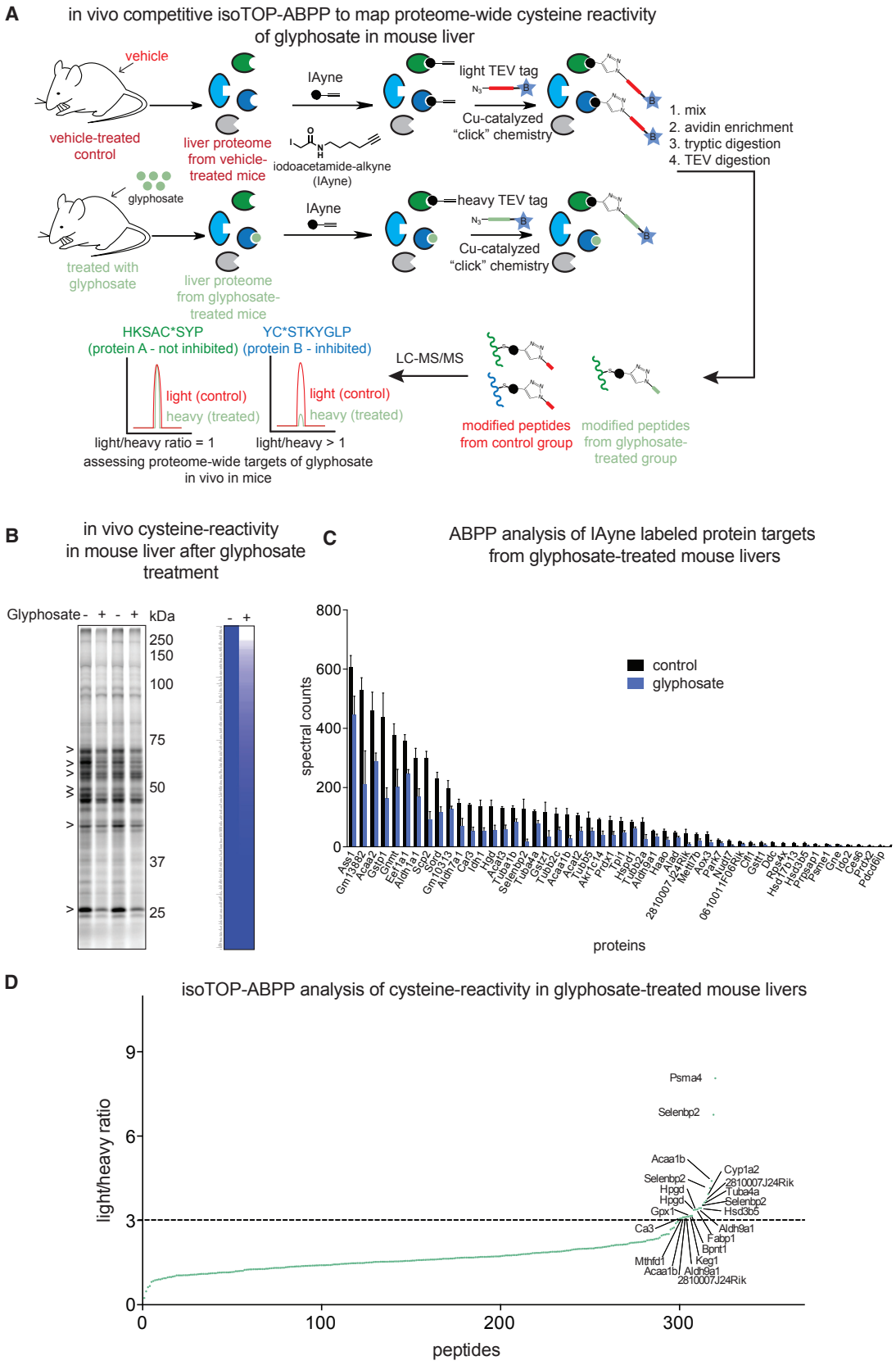

(legend on next page)

metabolites of glyphosate, we performed isotopic tandem orthogonal proteolysis-enabled ABPP (isoTOP-ABPP) to map proteome-wide cysteine reactivity of glyphosate and its metabolites in vivo in mouse liver (Weerapana et al., 2010) (Figure 2A). We labeled in vivo vehicle- and glyphosate-treated mouse liver proteomes with IAyne, followed by linking an isotopically light (vehicle) or heavy (glyphosate-treated) tobacco etch virus (TEV) recognition site-bearing biotin handle by click chemistry, combining the vehicle and glyphosate proteomes together in a 1:1 ratio, enriching IAyne-labeled proteins by biotin pull-down, tryptically digesting enriched proteins, and subsequently releasing the probe-modified tryptic peptides by TEV protease digestion. We identified >3,500 peptides bearing light or heavy IAyne-modified cysteines (Table S1). We quantitatively compared and interpreted only those peptides that were found in at least two of the three biological replicates. Among these resulting 320 cysteine-modified peptides, 190 showed >1.5, 67 showed >2, and 20 showed >3 light to heavy ratios (Figures 2D and 3A; Table S1). To determine whether these changes in ratios were dependent on changes in protein expression, we also performed standard proteomic profiling of vehicle- and glyphosate-treated liver proteomes. While 2810007J24Rik and Selenbp2 protein expression was significantly lower in glyphosate-treated mouse livers, we show that most of the protein targets that showed >3 light to heavy ratios did not show reduced protein expression, indicating that these targets are likely to be direct targets of glyphosate metabolites (Table S1). Among the top 21 modified peptides showing >3 light to heavy ratios, two of these cysteines corresponded to an annotated catalytic cysteine on Acaa1b (C123) and Aldh9a1 (C312) and one of these cysteines is an annotated glutathionylated site (C69) on Fabp1 (highlighted in red in Figure 3A), indicating that the function of these enzymes may be impaired by glyphosate or its metabolites in vivo (Chevillard et al., 2004; Dörmann et al., 1993; Riveros-Rosas et al., 2013). Acaa1b is a thiolase involved in peroxisomal fatty acid oxidation (Chevillard et al., 2004; Fidaleo et al., 2011). Aldh9a1 is an aldehyde dehydrogenase involved in the dehydrogenation of γ-aminobutyraldehyde to the neurotransmitter γ-aminobutyric acid (Lin et al., 1996). Fabp1 is a cytosolic fatty acid-binding protein involved in fatty acid transport and is a central regulator of whole-body metabolic control (Thumser et al., 2014).

We also mapped lysine reactivity using the previously described dichlorotriazine-alkyne (DCTyne) probe (Shannon et al., 2014). In mapping lysine reactivity with isoTOP-ABPP methods, we also identified three additional lysines annotated as known succinylation or acetylation sites on Hsd17b10 (K222), Cps1 (K1269), and Hbb-b1 (K145) that also showed light to heavy ratios >3 (Figure S2).

Mining deeper into our isoTOP-ABPP data, we also noticed that the peptides bearing catalytic cysteines for several thiolase family members also showed light to heavy ratios >1.5, including C92 of the mitochondrial fatty acid oxidation enzyme Acaa2, C94 of the peroxisomal fatty acid oxidation enzyme Scp2, and C92 of the cytosolic acetyl CoA acetyltransferase (Acat2) involved in biosynthesis of ketone bodies such as acetoacetyl-CoA (Figure 3B). As Acaa2, Acat2, and Scp2 protein expression was not significantly reduced upon glyphosate treatment (Table S1), we interpret these data to indicate that these cysteines are directly modified by glyphosate metabolites. We further show that glyoxylate displaces IAyne labeling of pure Acaa1b, Acaa2, and Scp2 in vitro and that glyoxylate also inhibits thiolase activities of Acaa1b and Acaa2 (Figures 3C and 3D). In addition, we performed isoTOP-ABPP analysis on in vitro glyoxylate cysteine reactivity in mouse liver proteomes and show that glyoxylate shows very similar reactivity signatures to those observed with in vivo glyphosate treatment, where we show that 141 of the 190 in vivo targets of glyphosate (74%) show >1.5 light to heavy ratios. This signature includes Acaa1b, Acaa2, and Scp2, which show >1.5 light to heavy ratios for nearly every probe-labeled site on these proteins for both in vitro glyoxylate and in vivo glyphosate treatments (Figure S3; Table S1).

Interestingly, Acaa1b, Acaa2, and Scp2 are all involved in mitochondrial or peroxisomal oxidation of long-chain and branched-chain fatty acids (Haapalainen et al., 2006). Genetic deficiencies in these thiolases or in peroxisomal or mitochondrial fatty acid oxidation pathways have been shown to cause liver dysfunction; lipid dysregulation in the form of elevated triacylglycerols, ceramides, and sterols; and hepatic steatosis, likely because the fatty acids that are not oxidized are diverted into other lipid metabolism pathways (Kim et al., 2014; Klipsic et al., 2015; Lee et al., 2016; Mizuno et al., 2013; Wanders et al., 2015).

We hypothesized that labeling of the catalytic cysteines on several thiolases involved in fatty acid oxidation would lead to the inhibition of these targets, impaired fatty acid oxidation, and diversion of fatty acids into other lipid pathways, including

Figure 2. ABPP Analysis of Ex Vivo Cysteine Reactivity in Mouse Liver from In Vivo Glyphosate Exposure

(A) Work flow for isoTOP-ABPP analysis. Mice were treated with glyphosate (200 mg/kg i.p., once per day for 7 days), and liver proteomes were treated with IAyne (100 μM) ex vivo, followed by click-chemistry-mediated appendage of a biotin tag bearing a TEV protease cleavage sequence and an isotopically light or heavy valine. Proteomes were combined, avidin enriched, and tryptically digested, and modified peptides were isolated by TEV digestion followed by quantitative proteomic analysis.

(B) Gel-based ABPP analysis of cysteine-reactivity profiling of liver proteomes from mice treated in vivo with vehicle or glyphosate. Proteomes were labeled with IAyne followed by click-chemistry-mediated appendage of rhodamine-azide or biotin-azide, followed by in-gel fluorescence or avidin enrichment and proteomic analysis. Arrows are pointing to IAyne-labeled bands that are lighter in glyphosate-treated groups. Shown are a representative gel and a heatmap showing IAyne-enriched protein targets, where dark blue indicates relative protein expression in control compared with that of glyphosate-treated mice. Light blue or white indicates proteins that showed reduced IAyne enrichment.

(C) Proteins that showed significantly ($p < 0.05$) reduced IAyne enrichment in livers from glyphosate-treated mice compared with vehicle-treated controls.

(D) isoTOP-ABPP analysis of IAyne-labeled peptides from vehicle-treated (light) and glyphosate-treated (heavy) mouse livers. Protein names for peptides showing light to heavy ratio >3 are designated.

Data in (C) are presented as means ± SEM, n = 3 mice/group. Iodoacetamide-rhodamine labeling data are shown in Figure S1. Protein expression profiling data are shown in Table S1. Lysine-reactivity data are shown in Figure S2. Raw and analyzed data from (B)–(D) can be found in Table S1. Figure 1 is related to Figures S1 and S2 and Table S1.

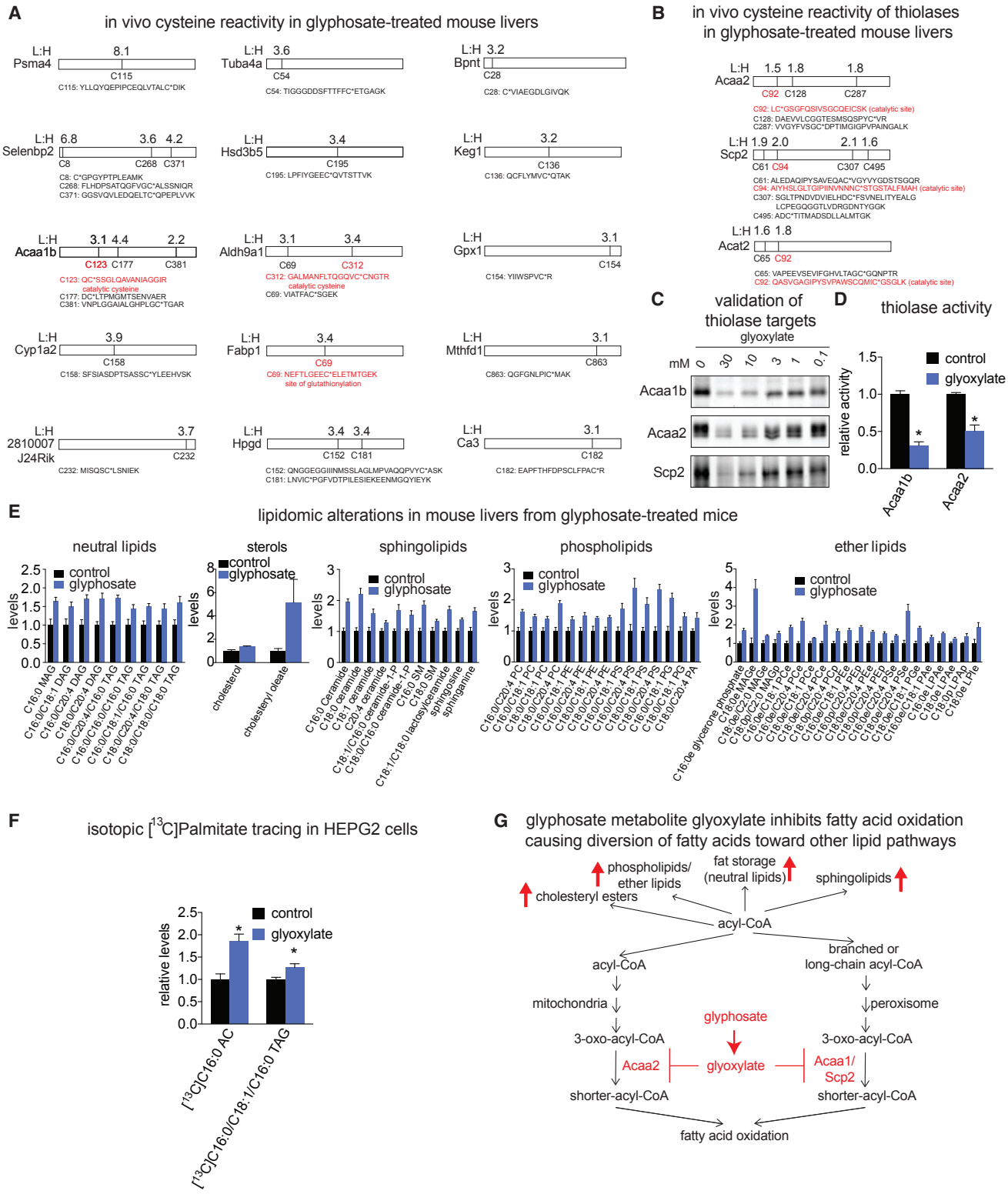

Figure 3. In Vivo Glyphosate Targets and Biochemical Changes in Mouse Liver

(A) Proteins from specific peptides that showed >3 light to heavy ratios from isoTOP-ABPP analysis of mouse livers from vehicle (light)- or glyphosate (heavy) (200 mg/kg i.p., once per day over 7 days)-treated mice. Specific cysteines labeled by IAyne, their corresponding tryptic peptide sequences and sites of modification, and light to heavy ratios of each protein are shown. Highlighted in red are catalytic cysteines (for Acaa1b and Aldh9a1) and the site of cysteine glutathionylation (for Fabp1).

(legend continued on next page)

triglycerides, sterols, and ceramides. We next performed a lipidomic profiling experiment in which we quantitatively measured the levels of 192 lipid and sterol species in vehicle- compared with glyphosate-treated mouse livers. We identified 62 distinct lipid species whose levels were significantly altered upon glyphosate treatment (Figure 3E; Table S2). These changes included elevations in several neutral lipids, including monoacylglycerols (MAGs), diacylglycerols (DAGs), and triacylglycerols (TAGs). We also observed increases in cholesterol and cholesteryl oleate levels as well as other lipid classes. Our data reveal that glyphosate treatment at high doses causes major lipid dysregulation, including increases in fat storage and cholesteryl esters in mouse liver (Figure 3E, Table S2). To further confirm our hypothesis, we also treated HEPG2 hepatocytes with glyoxylate and traced the fate of exogenously added isotopically labeled [^{13}C] palmitate and show that fatty acids are incorporated more into [^{13}C]palmitoyl carnitines (C16:0 AC) and [^{13}C]triacylglycerols (C16:0/C18:1/C16:0 TAG) (Figure 3F). These data are all consistent with our premise that inhibition of fatty acid oxidation enzymes by the glyphosate metabolite glyoxylate is associated with diversion of fatty acids into other lipid metabolism pathways.

We show here using both chemoproteomic and metabolomics approaches that glyphosate may be metabolized to reactive metabolites such as glyoxylate, which may react with and inhibit many cysteine-reactive protein targets in vivo in mouse liver, including several fatty acid oxidation enzymes, which may be associated with elevations in liver triacylglycerols, cholesteryl esters, and other lipid species (Figure 3G). We caution that the doses used in this study are much higher than any exposure levels encountered by the public and that further studies using lower doses in more relevant exposure paradigms will be necessary to fully evaluate these findings. Our data nonetheless show that glyphosate may be biotransformed to reactive metabolites that broadly react with key cysteines and lysines across many proteins in vivo, several of which are likely to cause dysfunction of those proteins and downstream physiological effects. Furthermore, while we identify glyoxylate as one possible metabolite of glyphosate that could be reactive, there may be additional reactive metabolites, which may explain the reactivity profiles observed in this study (Gohre et al., 1987). We also do not yet understand the tissues, cell types, and enzymes responsible for glyphosate metabolism and we cannot necessarily rule out the gut microbiome as a source for glyphosate metabolism into glyoxylate.

Nonetheless, our study provides much-needed mechanistic insights into the potential toxicities and toxicological mechanisms associated with glyphosate. Our data here show that in vivo glyphosate exposure may lead to generation of reactive metabolites such as glyoxylate, which may in turn inhibit fatty acid oxidation enzymes. We also show that glyphosate treatment at high doses is associated with heightened levels of triglycerides and cholesteryl esters and may potentially lead to corresponding metabolic disorders. Our results highlight the utility of using chemoproteomic platforms such as ABPP to map the proteome-wide reactivity and targets of environmental chemicals toward understanding their mechanisms of toxicity.

SIGNIFICANCE

In this study, we have used chemoproteomic and metabolomic platforms to map the direct targets and downstream metabolic consequences of glyphosate and its metabolites in vivo in mice, toward better understanding the potential toxicological mechanisms of this active ingredient found in the very widely used herbicide Roundup. We show that glyphosate is metabolized in vivo to a reactive metabolite, glyoxylate, at high doses in mice, where it reacts with many protein targets. We show that fatty acid oxidation enzymes are inhibited by glyoxylate and that glyphosate treatment in mice leads to elevated levels of fat and cholesteryl esters in the liver.

EXPERIMENTAL PROCEDURES

Mice

Male C57BL/6 mice (6–8 weeks old) were acutely (2 hr) or subacutely (7 days) exposed by i.p. injection to 200 mg/kg glyphosate (Sigma 45521) in a vehicle of PBS (10 μL/g mouse weight). Following exposure, mice were sacrificed by cervical dislocation, and liver and serum were immediately removed and flash frozen in liquid nitrogen. Animal experiments were conducted in accordance with the guidelines of the Institutional Animal Care and Use Committee of the University of California, Berkeley.

Processing of Mouse Liver Proteomes

Tissues were homogenized in PBS, followed by a 1,000 × *g* centrifugation of the homogenate. The resulting supernatant was collected and used for subsequent assays. Protein concentrations were determined by BCA protein assay (Pierce).

Activity Assays

Enzymatic activity of Acaa1b and Acaa2 was performed using the Fluorometric Acetyltransferase Activity Assay Kit (Abcam ab204536). The assay was performed per the protocol with 0.4 μg of pure protein, 3 mM glyoxylate, and 100 nM acetoacetyl-CoA (Sigma A1625); fluorescence was measured at 380/520 ex/em on a SpectraMax i3x detection platform.

Proteomic Analysis

For ABPP and isoTOP-ABPP analysis, we performed studies as previously described (Medina-Cleghorn et al., 2015; Weerapana et al., 2010). Detailed procedures are described in the Supplemental Experimental Procedures.

(B) Shown is an equivalent analysis for other members of the thiolase family.
(C) Glyoxylate competition study against IAyne labeling of pure human Acaa1b, Acaa2, and Scp2 analyzed by in-gel fluorescence.
(D) Thiolase activity assay using pure mouse Acaa1b and Acaa2 protein showing that incubation of pure protein with gloxylate (3 mM) inhibits thiolase activity.
(E) Significant changes ($p < 0.05$) in metabolites from lipidomic profiling of vehicle- versus glyphosate-treated mouse livers.
(F) Isotopic [^{13}C]C16:0 FFA tracing in HEPG2 cells. Cells were pretreated with glyoxylate (1 mM) for 1 hr prior to labeling cells with [^{13}C]C16:0 FFA (10 mM) for 6 hr. Isotopically labeled triglycerides were measured using SRM-based LC-MS/MS.
(G) Diagram showing how glyphosate metabolites inhibit thiolases involved in peroxisomal and mitochondrial fatty acid oxidation, leading to accumulation of fatty acids in other lipid and sterol species. Glyoxylate cysteine-reactivity data are shown in Figure S3 and Table S1.
Data in (E and F) are presented as the mean ± SEM, n = 5/group. Significance in (F) is presented as *$p < 0.05$ compared with vehicle-treated control.

Metabolomic Profiling

Metabolomic profiling was performed as previously described (Benjamin et al., 2013; Louie et al., 2016). Detailed methods are described in the Supplemental Experimental Procedures.

SUPPLEMENTAL INFORMATION

Supplemental Information includes Supplemental Experimental Procedures, three figures, and two tables and can be found with this article online at http://dx.doi.org/10.1016/j.chembiol.2016.12.013.

AUTHOR CONTRIBUTIONS

B.F. and D.K.N. performed experiments, interpreted data, and wrote the paper; L.A.B. and L.G.P. performed experiments; R.P. provided bioinformatics support for analyzing the quantitative proteomics data.

ACKNOWLEDGMENTS

We thank Michelle Luu and Joseph Hendricks for assistance on this project. We also thank members of the Nomura Research Group and colleagues for careful reading of the manuscript. This work was supported by a Searle Scholar Award and the Center for Environmental Research on Toxics.

Received: August 19, 2016
Revised: November 14, 2016
Accepted: December 21, 2016
Published: January 26, 2017

REFERENCES

Benjamin, D.I., Cozzo, A., Ji, X., Roberts, L.S., Louie, S.M., Mulvihill, M.M., Luo, K., and Nomura, D.K. (2013). Ether lipid generating enzyme AGPS alters the balance of structural and signaling lipids to fuel cancer pathogenicity. Proc. Natl. Acad. Sci. USA *110*, 14912–14917.

Chang, E.T., and Delzell, E. (2016). Systematic review and meta-analysis of glyphosate exposure and risk of lymphohematopoietic cancers. J. Environ. Sci. Health B *51*, 402–434.

Chevillard, G., Clémencet, M.-C., Etienne, P., Martin, P., Pineau, T., Latruffe, N., and Nicolas-Francès, V. (2004). Molecular cloning, gene structure and expression profile of two mouse peroxisomal 3-ketoacyl-CoA thiolase genes. BMC Biochem. *5*, 3.

Counihan, J.L., Ford, B., and Nomura, D.K. (2015). Mapping proteome-wide interactions of reactive chemicals using chemoproteomic platforms. Curr. Opin. Chem. Biol. *30*, 68–76.

Cressey, D. (2015). Widely used herbicide linked to cancer. Nature. http://dx.doi.org/10.1038/nature.2015.17181.

Dörmann, P., Börchers, T., Korf, U., Højrup, P., Roepstorff, P., and Spener, F. (1993). Amino acid exchange and covalent modification by cysteine and glutathione explain isoforms of fatty acid-binding protein occurring in bovine liver. J. Biol. Chem. *268*, 16286–16292.

El-Shenawy, N.S. (2009). Oxidative stress responses of rats exposed to Roundup and its active ingredient glyphosate. Environ. Toxicol. Pharmacol. *28*, 379–385.

Fidaleo, M., Arnauld, S., Clémencet, M.-C., Chevillard, G., Royer, M.-C., De Bruycker, M., Wanders, R.J.A., Athias, A., Gresti, J., Clouet, P., et al. (2011). A role for the peroxisomal 3-ketoacyl-CoA thiolase B enzyme in the control of PPARα-mediated upregulation of SREBP-2 target genes in the liver. Biochimie *93*, 876–891.

Gohre, K., Casida, J.E., and Ruzo, L.O. (1987). N-oxidation and cleavage of the amino acid derived herbicide glyphosate and anilino acid of the insecticide fluvalinate. J. Agric. Food Chem. *35*, 388–392.

Greim, H., Saltmiras, D., Mostert, V., and Strupp, C. (2015). Evaluation of carcinogenic potential of the herbicide glyphosate, drawing on tumor incidence data from fourteen chronic/carcinogenicity rodent studies. Crit. Rev. Toxicol. *45*, 185–208.

Grube, A., Donaldson, D., Kiely, T., and Wu, L. (2011). Pesticides Industry Sales and Usage: 2006 and 2007 Market Estimates (US EPA).

Haapalainen, A.M., Meriläinen, G., and Wierenga, R.K. (2006). The thiolase superfamily: condensing enzymes with diverse reaction specificities. Trends Biochem. Sci. *31*, 64–71.

International Agency for Research on Cancer. (2015). IARC Monographs on the Evaluation of Carcinogenic Risks to Humans, Volume 115. Some Organophosphate Insecticides and Herbicides: Diazinon, Glyphosate, Malathion, Parathion, and Tetrachlorvinphos. http://monographs.iarc.fr/ENG/Monographs/vol112/mono112-09.pdf.

Kim, T., Moore, J.F., Sharer, J.D., Yang, K., Wood, P.A., and Yang, Q. (2014). Carnitine palmitoyltransferase 1b deficient mice develop severe insulin resistance after prolonged high fat diet feeding. J. Diabetes Metab. *5*, http://dx.doi.org/10.4172/2155-6156.1000401.

Klipsic, D., Landrock, D., Martin, G.G., McIntosh, A.L., Landrock, K.K., Mackie, J.T., Schroeder, F., and Kier, A.B. (2015). Impact of SCP-2/SCP-x gene ablation and dietary cholesterol on hepatic lipid accumulation. Am. J. Physiol. Gastrointest. Liver Physiol. *309*, G387–G399.

Lee, J., Choi, J., Scafidi, S., and Wolfgang, M.J. (2016). Hepatic fatty acid oxidation restrains systemic catabolism during starvation. Cell Rep. *16*, 201–212.

Lin, S.W., Chen, J.C., Hsu, L.C., Hsieh, C.L., and Yoshida, A. (1996). Human gamma-aminobutyraldehyde dehydrogenase (ALDH9): cDNA sequence, genomic organization, polymorphism, chromosomal localization, and tissue expression. Genomics *34*, 376–380.

Louie, S.M., Grossman, E.A., Crawford, L.A., Ding, L., Camarda, R., Huffman, T.R., Miyamoto, D.K., Goga, A., Weerapana, E., and Nomura, D.K. (2016). GSTP1 is a driver of triple-negative breast cancer cell metabolism and pathogenicity. Cell Chem. Biol. *23*, 567–578.

Medina-Cleghorn, D., Bateman, L.A., Ford, B., Heslin, A., Fisher, K.J., Dalvie, E.D., and Nomura, D.K. (2015). Mapping proteome-wide targets of environmental chemicals using reactivity-based chemoproteomic platforms. Chem. Biol. *22*, 1394–1405.

Mesnage, R., Arno, M., Costanzo, M., Malatesta, M., Séralini, G.-E., and Antoniou, M.N. (2015). Transcriptome profile analysis reflects rat liver and kidney damage following chronic ultra-low dose Roundup exposure. Environ. Health Glob. Access Sci. Source *14*, 70.

Mizuno, Y., Ninomiya, Y., Nakachi, Y., Iseki, M., Iwasa, H., Akita, M., Tsukui, T., Shimozawa, N., Ito, C., Toshimori, K., et al. (2013). Tysnd1 deficiency in mice interferes with the peroxisomal localization of PTS2 enzymes, causing lipid metabolic abnormalities and male infertility. PLoS Genet. *9*, e1003286.

Monsanto. (2015). Monsanto Disagrees with IARC Classification for Glyphosate (Monsanto Newsroom). http://news.monsanto.com/news/monsanto-disagrees-iarc-classification-glyphosate.

Portier, C.J., Armstrong, B.K., Baguley, B.C., Baur, X., Belyaev, I., Bellé, R., Belpoggi, F., Biggeri, A., Bosland, M.C., Bruzzi, P., et al. (2016). Differences in the carcinogenic evaluation of glyphosate between the International Agency for Research on Cancer (IARC) and the European Food Safety Authority (EFSA). J. Epidemiol. Community Health *70*, 741–745.

Riveros-Rosas, H., González-Segura, L., Julián-Sánchez, A., Díaz-Sánchez, A.G., and Muñoz-Clares, R.A. (2013). Structural determinants of substrate specificity in aldehyde dehydrogenases. Chem. Biol. Interact. *202*, 51–61.

Roberts, A.M., Ward, C.C., and Nomura, D.K. (2016). Activity-based protein profiling for mapping and pharmacologically interrogating proteome-wide ligandable hotspots. Curr. Opin. Biotechnol. *43*, 25–33.

Samsel, A., and Seneff, S. (2015). Glyphosate, pathways to modern diseases IV: cancer and related pathologies. J. Biol. Phys. Chem. *15*, 121–159.

Schuette, J. (1998). Environmental Fate of Glyphosate (California: Department of Pesticide Regulation).

Shannon, D.A., Banerjee, R., Webster, E.R., Bak, D.W., Wang, C., and Weerapana, E. (2014). Investigating the proteome reactivity and selectivity of aryl halides. J. Am. Chem. Soc. *136*, 3330–3333.

Thumser, A.E., Moore, J.B., and Plant, N.J. (2014). Fatty acid binding proteins: tissue-specific functions in health and disease. Curr. Opin. Clin. Nutr. Metab. Care *17*, 124–129.

Wanders, R.J.A., Waterham, H.R., and Ferdinandusse, S. (2015). Metabolic interplay between peroxisomes and other subcellular organelles including mitochondria and the endoplasmic reticulum. Front. Cell Dev. Biol. *3*, 83.

Wang, W., Wu, Z., Dai, Z., Yang, Y., Wang, J., and Wu, G. (2013). Glycine metabolism in animals and humans: implications for nutrition and health. Amino Acids *45*, 463–477.

Weerapana, E., Wang, C., Simon, G.M., Richter, F., Khare, S., Dillon, M.B.D., Bachovchin, D.A., Mowen, K., Baker, D., and Cravatt, B.F. (2010). Quantitative reactivity profiling predicts functional cysteines in proteomes. Nature *468*, 790–795.

Williams, G.M., Kroes, R., and Munro, I.C. (2000). Safety evaluation and risk assessment of the herbicide Roundup and its active ingredient, glyphosate, for humans. Regul. Toxicol. Pharmacol. *31*, 117–165.

Cell Chemical Biology, Volume *24*

Supplemental Information

Mapping Proteome-wide Targets of Glyphosate in Mice

Breanna Ford, Leslie A. Bateman, Leilani Gutierrez-Palominos, Robin Park, and Daniel K. Nomura

Supporting Information

Mapping Proteome-Wide Targets of Glyphosate in Mice

Breanna Ford[1], Leslie A. Bateman[1], Leilani Gutierrez-Palominos[1], Robin Park[2], Daniel K. Nomura*[1]

[1] Departments of Chemistry, Molecular and Cell Biology, and Nutritional Sciences and Toxicology, 127 Morgan Hall, University of California, Berkeley, Berkeley, CA 94720

[2] Integrated Proteomics Applications, Inc., 12707 High Bluff Dr. Suite 200, San Diego, CA 92130

*correspondence to dnomura@berkeley.edu

Supplemental Methods

Cell Culture and Pure Proteins. HEK293T were cultured in DMEM media containing 10% FBS and maintained at 37°C with 5% CO_2. Pure human Acaa1b, Acaa2, and Scp2 proteins were purchased from Origene.

Proteomic analysis

For ABPP analysis of IAyne labeled proteins, proteome samples from control or glyphosate treated mice were diluted (1 mg diluted in 500uL PBS) then labeled with IAyne (10 μM) for 1 hour at room temperature. We added the biotin azide to IAyne labeled proteins through click chemistry by sequential addition of tris(2-carboxyethyl)phosphine (1 mM, Sigma-Aldrich), copper (II) sulfate (1 mM, Sigma-Aldrich), tris[(1-benzyl-1H-1,2,3-triazol-4-yl)methyl]amine (34 μM, Sigma-Aldrich) using previously described methods (Nomura et al., 2010; Weerapana et al., 2010). After click reactions, proteomes were precipitated by centrifugation at 6500 x *g*, washed twice in ice-cold methanol, then denatured and resolubilized by heating in 1.2% SDS/PBS to 85ºC for 5 minutes. Insoluble components were precipitated by centrifugation at 6500 x *g* and soluble proteome was diluted in 5 ml PBS, for a final concentration of 0.2% SDS. Labeled proteins were bound to avidin-agarose beads (170 μL resuspended beads/sample, Thermo Pierce) while rotating overnight at 4ºC. Bead-linked proteins were enriched by washing three times each in PBS and water, then resuspended in 6 M urea/PBS (Sigma-Aldrich) and reduced in dithiothreitol (1 mM, Sigma-Aldrich), alkylated with iodoacetamide (18 mM, Sigma-Aldrich), then washed and resuspended in 2 M urea and trypsinized overnight with 0.5 μg/μl sequencing grade trypsin (Promega). Tryptic peptides were diluted in water and acidified with final concentration of 5% formic acid (1.2 M, Spectrum).

For isoTOP-ABPP analysis, proteomes labeled with IAyne or DCTyne (100 μM) for 1 h at room temperature, and were subsequently treated with 100 μM isotopically light (control) or heavy (treated) TEV-biotin and click chemistry was performed as previously described (Nomura et al., 2010; Weerapana et al., 2010). Proteins were precipitated over one hour and pelleted by centrifugation at 6500 x *g.* Proteins were washed 3 times with cold methanol then denatured and resolubilized by heating in 1.2% SDS/PBS to 85ºC for 5 minutes. Insoluble components were precipitated by centrifugation at 6500 x *g* and soluble proteome was diluted in 5 ml PBS, for a final concentration of 0.2% SDS. Labeled proteins were bound to avidin-agarose

beads (170 μL resuspended beads/sample, Thermo Pierce) while rotating overnight at 4ºC. Bead-linked proteins were enriched by washing three times each in PBS and water, then resuspended in 6 M urea/PBS (Sigma-Aldrich) and reduced in dithiothreitol (1 mM, Sigma-Aldrich), alkylated with iodoacetamide (18 mM, Sigma-Aldrich), then washed and resuspended in 2 M urea/PBS with 1mM calcium chloride and trypsinized overnight with 0.5 ug/ul sequencing grade trypsin (Promega). Tryptic pepetides were discarded and beads were washed three times each in PBS and water, then washed with one wash of TEV buffer containing 1 μM DTT. TEV-biotin tag was digested overnight in TEV buffer containing 1 μM DTT and 5 μL Ac-TEV protease at 29ºC. Peptides were diluted in water and acidified with final concentration of 5% formic acid (1.2 M, Spectrum).

Shotgun proteomic samples were prepared by precipitating proteomes using 100% trichloroacetic acid (sigma T6399), which was added to a final concentration of 20%. Samples were incubated at -80ºC overnight to precipitate proteins and then centrifuged at 4ºC for 10 min at 10,000 g. The pellet was washed 3 times with ice cold 0.1 M HCl in 90% acetone, air-dried and then resuspended in 30 μL 8M urea in PBS. Protease max (30 μL of 0.2% in 100 mM ammonium bicarbonate) was added to samples, followed by vortexing and dilution with 40 μL ammonium bicarbonate. TCEP was added to a final concentration of 10 mM and then samples were incubated for 30 min at 60ºC, followed by addition of iodoacetamide to a final concentration of 12.5 mM, and samples were incubated in foil at room temp for 30 min. Samples were diluted with 100 μL of PBS and 1.2 μL of 1% protease max was added and vortexed well, after which 2 μg sequencing trypsin was added and samples incubated overnight at 37ºC. Trypsinized samples were acidified with 5% final concentration formic acid and centrifuged at 13200 rpm for 30min.

Peptides from all proteomic experiments were pressure-loaded onto a 250 mm i.d. fused silica capillary tubing packed with 4 cm of Aqua C18 reverse-phase resin (phenomenex # 04A-4299) which was previously equilibrated on an Agilent 600 series HPLC using gradient from 100% buffer A to 100% buffer B over 10 min, followed by a 5 min wash with 100% buffer B and a 5 min wash with 100% buffer A. The samples were then attached using a MicroTee PEEK 360 μm fitting (Thermo Fisher Scientific #p-888) to a 10 cm laser pulled column of 100 mm fused silica capillary packed with 10 cm Aqua C18 reverse-phase resin for shotgun proteomics and ABPP studies, or to a 13 cm laser pulled column packed with 10 cm Aqua C18 reverse-phase resin and 3 cm of strong-cation exchange resin (Multidimensional Protein Identification Technology (MudPIT)

column) for isoTOP-ABPP studies. Samples were analyzed using an Orbitrap Q Exactive Plus mass spectrometer (Thermo Fisher Scientific). Data was collected in data-dependent acquisition mode with dynamic exclusion enabled (60 s). One full MS (MS1) scan (400-1800 m/z) was followed by 15 MS2 scans (ITMS) of the nth most abundant ions. Heated capillary temperature was set to 200ºC and the nanospray voltage was set to 2.75kV.

For 1D runs for shotgun proteomics and ABPP studies, samples were run using a two hour gradient from 5 % to 80 % acetonitrile with 0.1 % formic acid at 100 nl/min. For MudPIT runs, samples were run with the following 5-step MudPIT program (using 0%, 10%, 25%, 80%, and 100% salt bumps). Data was extracted in the form of MS1 and MS2 files using Raw Extractor 1.9.9.2 (Scripps Research Institute) and searched against the Uniprot mouse database using ProLuCID search methodology in IP2 v.3 (Integrated Proteomics Applications, Inc) (Xu et al., 2015). Cysteine residues were searched with a static modification for carboxyaminomethylation (+57.02146) and up to two differential modifications for either the light or heavy TEV tags (+464.28596 or +470.29977, respectively). Peptides were required to have at least one tryptic end and to contain the TEV modification. ProLUCID data was filtered through DTASelect to achieve a peptide false-positive rate below 1%.

Metabolomic Profiling

Nonpolar lipid metabolites from the liver or serum of *in vivo* treated mice were extracted in 3 ml of 2:1 chloroform:methanol and 1 ml of PBS with inclusion of internal standards C12:0 monoalkylglycerol ether (MAGE) (10 nmol, Santa Cruz Biotechnology) and pentadecanoic acid (10 nmol, Sigma-Aldrich). Organic and aqueous layers were separated by centrifugation at 1000 x *g* for 5 min and the organic layer was collected, dried under a stream of N_2 and dissolved in 120 μl chloroform. An aliquot was injected onto LC/MS. Polar metabolites, such as glyphosate, AMPA, and glyoxylate, were extracted in 500 μl of 40:40:20 (acetonitrile:methanol:water) with inclusion of internal standard d_3N^{15}-serine (Cambridge Isotope Laboratories, Inc. #DNLM-6863). Samples were centrifuged at 10,000 x g for 10 min and an aliquot of the supernatant was injected onto LC/MS. Metabolites were separated by liquid chromatography as previously described (Louie et al., 2016). MS analysis was performed with an electrospray ionization (ESI) source on an Agilent 6430 QQQ LC-MS/MS (Agilent Technologies). The capillary voltage was set to 3.0 kV, and the fragmentor voltage was set

to 100 V. The drying gas temperature was 350°C, the drying gas flow rate was 10 l/min, and the nebulizer pressure was 35 psi. Metabolites were identified by SRM of the transition from precursor to product ions at associated optimized collision energies and retention times as previously described (Benjamin et al., 2013; Louie et al., 2016). All metabolites measured in this paper including lipid metabolites and glyphosate and glyphosate metabolites were subjected to fragmentation analysis to yield the specific SRM targeted LC-MS/MS programs and we have confirmed that the retention times of standards matches the retention times of metabolites found in tissues. For lipidomics, SRM programs and confirmation of retention times were already performed in previous studies (Benjamin et al., 2013; Louie et al., 2016). For glyphosate and its metabolites, the SRMs and retention times used are noted in **Fig. 1A.** Metabolites were quantified by integrating the area under the curve, then normalized to internal standard values and tissue weight. Metabolite levels are expressed as relative abundances as compared to controls.

Glyoxylate Competition, Click Chemistry and In-Gel Fluorescence Imaging. Proteome samples diluted in PBS (50 μg in 50 μl PBS) were subjected to vehicle or glyoxylate treatment for 30 min at 37ºC, (glyoxylate solution was adjusted to pH 7 prior to incubation). Then, IAyne (10 μM, CHESS Gmbh # 3187) or IA-Rhodamine (IA-Rh, Life Technologies Corporation #T6006) labeling was performed for 30 min at 37ºC. Copper-catalyzed azide-alkyne cycloaddition “click chemistry” was performed to append rhodamine-azide onto IAyne probe-labeled proteins using previously described methods (Medina-Cleghorn et al., 2015). Proteomes were separated on by SDS-PAGE and scanned using a ChemiDoc MP (Bio-Rad Laboratories, Inc). Inhibition of target labeling was assessed by densitometry using ImageLab software 5.2.1 (Bio-Rad Laboratories, Inc) and regressions were calculated by Prism (GraphPad Software).

Supplemental References

Benjamin, D.I., Cozzo, A., Ji, X., Roberts, L.S., Louie, S.M., Mulvihill, M.M., Luo, K., and Nomura, D.K. (2013). Ether lipid generating enzyme AGPS alters the balance of structural and signaling lipids to fuel cancer pathogenicity. Proc. Natl. Acad. Sci. U. S. A. *110*, 14912–14917.

Louie, S.M., Grossman, E.A., Crawford, L.A., Ding, L., Camarda, R., Huffman, T.R., Miyamoto, D.K., Goga, A., Weerapana, E., and Nomura, D.K. (2016). GSTP1 is a Driver of Triple-Negative Breast Cancer Cell Metabolism and Pathogenicity. Cell Chem. Biol. *In press*.

Xu, T., Park, S.K., Venable, J.D., Wohlschlegel, J.A., Diedrich, J.K., Cociorva, D., Lu, B., Liao, L., Hewel, J., Han, X., et al. (2015). ProLuCID: An improved SEQUEST-like algorithm with enhanced sensitivity and specificity. J. Proteomics *129*, 16–24.

Supplemental Table Legends

Table S1. Chemoproteomic profiling of *in vivo* glyphosate reactivity in mouse liver. Tabs 1-3. Enrichment of IAyne-labeled proteins from livers from mice treated with vehicle or glyphosate. Proteomes were labeled with IAyne, followed by appendage of biotin-azide by click-chemistry, avidin enrichment, tryptic digestion, and analysis by LC-MS/MS. **Tab 1** shows raw proteomic data, **Tab 2** shows enriched IAyne-labeled proteins that show >3 spectral counts, and **Tab 3** shows those proteins that showed significantly less IAyne labeling in glyphosate-treated mouse livers compared to their control counterparts. **Tabs 4-9.** isoTOP-ABPP analysis of IAyne cysteine-reactivity in mouse livers from mice treated with vehicle or glyphosate. Proteomes were labeled with IAyne, followed by appendage of a biotin-azide handle bearing a TEV recognition sequence and isotopically light (vehicle-treated) or heavy (glyphosate-treated) valine, combining of control and treated proteomes in a 1:1 ratio, avidin enrichment, tryptic digestion, release of modified peptides by TEV protease, and analysis by LC-MS/MS. Shown are modified peptides and their corresponding protein IDs that were quantified by measuring the light to heavy ratios of peptides. Specific modified cysteines are presented as C(464.28596) or C(470.29977) or C*. **Tabs 4-6** show the raw proteomic data, **Tab 7** shows all peptides quantified, **Tab 8** shows averaging of ratios for redundant peptides, **Tab 9** shows final ratios for modified peptides. **Tab 10-12** Shotgun proteomics data showing protein expression of proteins in mouse liver proteomes from mice treated with vehicle or glyphosate. **Tab 10** shows the raw proteomic data, **Tab 11** shows those proteins that had an average of 3 spectral counts, **Tab 12** are the relative expression of proteins that were identified as having >3 light:heavy ratios from the isoTOP-ABPP analysis or proteins in the thiolase family that were also detected by shotgun proteomics. **Tab 13** shows isoTOP-ABPP analysis of glyoxylate cysteine-reactivity from *in vitro* pre-treatment with glyoxylate (3 mM, 30 min) prior to labeling with IAyne followed by appendage of a biotin-azide handle bearing a TEV recognition sequence and isotopically light (vehicle-treated) or heavy (glyphosate-treated) valine, combining of control and treated proteomes in a 1:1 ratio, avidin enrichment, tryptic digestion, release of modified peptides by TEV protease, and analysis by LC-MS/MS. Shown are modified peptides and their corresponding protein IDs that were quantified by measuring the light to heavy ratios of peptides. **Tab 14** shows the target list for glyphosate (>1.5 L:H ratio) and those peptides that also showed >1.5 L:H ratios with glyoxylate isoTOP-ABPP analysis from **Tab 13.** This table is related to **Figure 2.**

Mice from all studies in this table were treated with vehicle or glyphosate (200 mg/kg ip, once per day treatment over 7 days).

Table S2. Lipidomic profiling of mouse livers from mice treated with vehicle or glyphosate. Mice were treated with vehicle or glyphosate (200 mg/kg ip, once per day treatment over 7 days). Relative metabolite levels from individual mice are presented where the data for each lipid is normalized to "1" for vehicle-treated controls. Abbreviations for lipids are as followed: FFA, free fatty acid; PA, phosphatidic acid; PS, phosphatidyl serine; PE, phosphatidylethanolamine; PC, phosphatidylcholine; PG, phosphatidylglycerol; PI, phosphatidyl inositol; SM, sphingomyelin; AC, acyl carnitine; NAE, N-acylethanolamine; MAG, monoacylglycerol; DAG, diacylglycerol; TAG, triacylglycerol; PGE2/PGD2, prostaglandin E2/D2; PGJ2, prostaglandin J2; 5,6-EET, 5,6-epoxyeicosatrienoic acid; 5-HETE, 5-hydroxyeicosatetraenoic acid; PGF2alpha, prostaglandin F2-alpha; NAT, N-acyltaurine; TXB2, thromboxane B2; S1P, sphingosine-1-phosphate; "L" in front of a lipid acronym refers to "lyso" (e.g. LPA refers to lysophosphatidic acid); "e" or "p" after a lipid acronym refers to ether or plasmalogen, respectively. This table is related to **Figure 3.**

Supplemental Figures

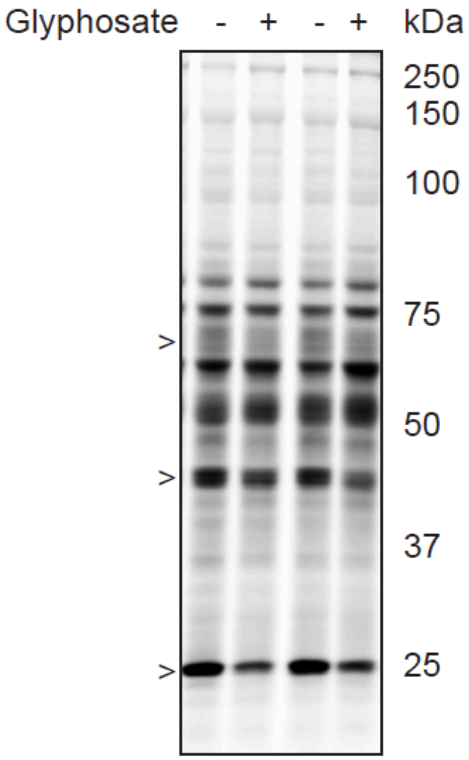

Figure S1. Iodoacetamide-rhodamine labeling of mouse liver proteomes from mice treated with vehicle or glyphosate. Mice were treated with vehicle or glyphosate (200 mg/kg ip, once per day treatment over 7 days). Liver proteomes were labeled with iodoacetamide-rhodamine, and analyzed by in-gel fluorescence. “>”s refer to probe-labeled proteins that are decreased in signal in glyphosate-treated mouse livers. Study was done with n=3 mice/group and shown are representative gels. **Fig. S1** is related to **Figure 2.**

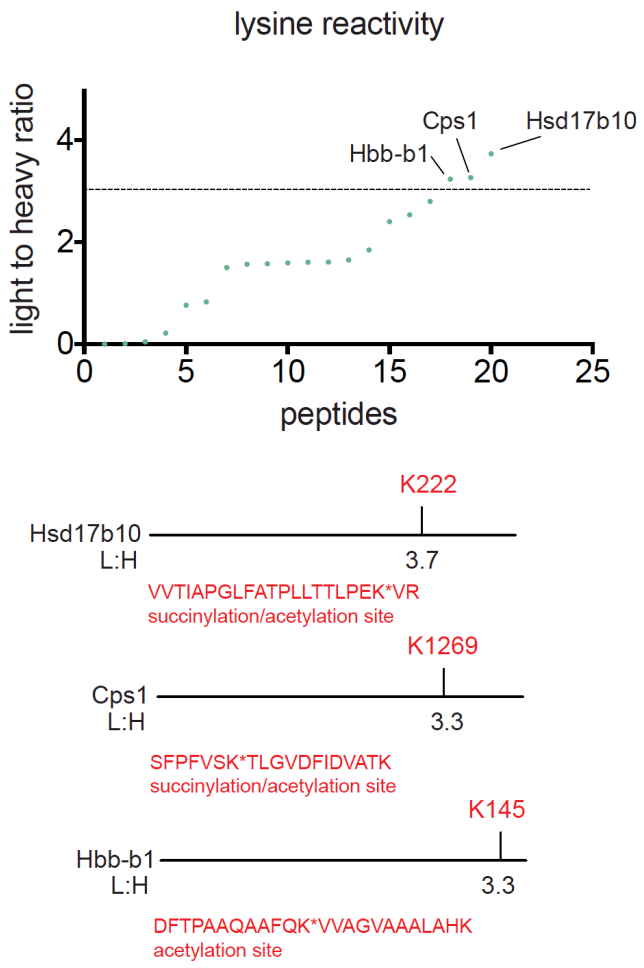

Figure S2. isoTOP-ABPP analysis of DCTyne lysine-reactivity in mouse livers from mice treated with vehicle or glyphosate. Proteomes were labeled with DCTyne, followed by appendage of a biotin-azide handle bearing a TEV recognition sequence and isotopically light (vehicle-treated) or heavy (glyphosate-treated) valine, combining of control and treated proteomes in a 1:1 ratio, avidin enrichment, tryptic digestion, release of modified peptides by TEV protease, and analysis by LC-MS/MS. Shown are light:heavy ratios of modified peptides and highlighted are those proteins and specific modified peptides that showed >3 light:heavy ratio. Data and ratios are from 3 mice/group. **Fig. S2** is related to **Figure 2.**

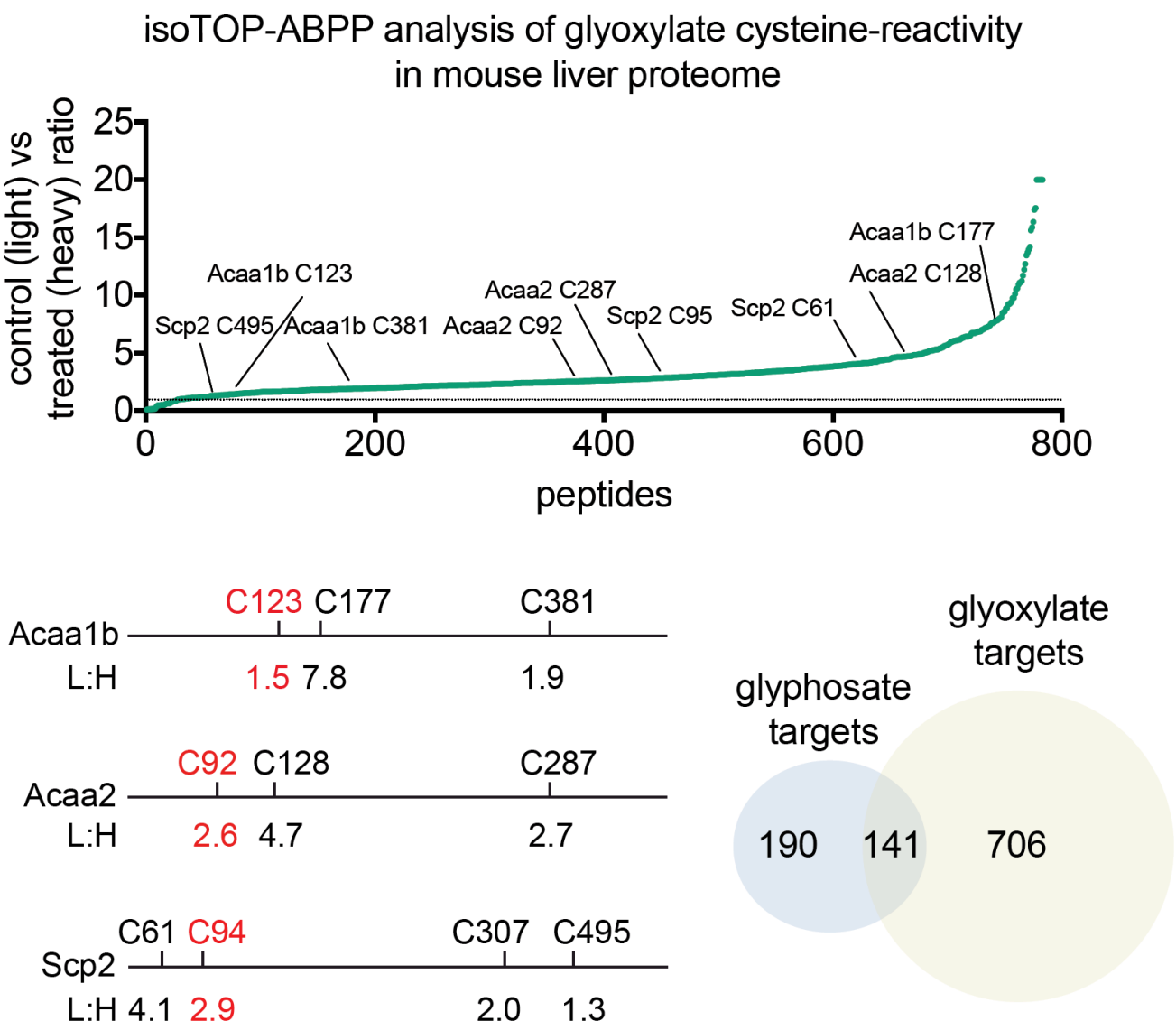

Figure S3. isoTOP-ABPP analysis of glyoxylate cysteine-reactivity in mouse livers. Proteomes were pre-treated with glyoxylate (3 mM, 30 min) prior to labeling with IAyne, followed by appendage of a biotin-azide handle bearing a TEV recognition sequence and isotopically light (vehicle-treated) or heavy (glyphosate-treated) valine, combining of control and treated proteomes in a 1:1 ratio, avidin enrichment, tryptic digestion, release of modified peptides by TEV protease, and analysis by LC-MS/MS. Shown are average light:heavy ratios of modified peptides and modified peptides of Acaa1b, Acaa2, and Scp2 and their light to heavy ratios. Highlighted in red are the catalytic cysteines of Acaa1b, Acaa2, and Scp2. Also shown graphically are the number of glyphosate *in vivo* targets (190), glyoxylate *in vitro* targets (706), and overlapping targets (141) in mouse liver that showed >1.5 light:heavy ratios. Data and average ratios are from n=3 experiments. **Fig. S3** is related to **Figure 3.**